Sensors and Materials, Vol. 35, No. 2 (2023) 429–437
MYU Tokyo

S & M 3179

Photoluminescence and Scintillation Properties of Ce-doped $(Mg_xCa_{1-x})HfO_3$ Single Crystals

Hiroyuki Fukushima,* Daisuke Nakauchi, Takumi Kato,
Noriaki Kawaguchi, and Takayuki Yanagida

Division of Materials Science, Nara Institute of Science and Technology,
8916-5 Takayama-cho, Ikoma, Nara 630-0192, Japan

(Received September 29, 2022; accepted January 10, 2023)

Keywords: scintillation, photoluminescence, single crystal, floating zone

Ce:$(Mg_xCa_{1-x})HfO_3$ (x = 0.5, 2.5, 5, and 10%) single crystals were successfully grown by the floating zone method, and their photoluminescence (PL) and scintillation properties were investigated. A broad luminescence band with a maximum at 430 nm was observed in both the PL and scintillation spectra. The PL quantum yield (*QY*) improved with the substitution of Mg, and the PL *QY* of Ce:$(Mg_xCa_{1-x})HfO_3$ reached 50%. Fast decay due to the 5d–4f transition of Ce^{3+} was observed for both the PL and scintillation. Ce:$(Mg_xCa_{1-x})HfO_3$ (x = 5%) showed the highest light yield of ~9500 photons/MeV among the synthesized samples, and this value is higher than that of common X- and gamma-ray detection scintillators such as $Bi_4Ge_3O_{12}$ and Ce:Gd_2SiO_5 single crystals.

1. Introduction

A scintillator converts high-energy ionizing radiation to low-energy luminescence. A primary electron is generated when a material absorbs the energy of ionizing radiation, then many secondary electrons are generated by an interaction with the host lattice. Subsequently, electron–hole pairs are created and, finally, electrons and holes recombine at luminescence centers. The typical applications of scintillators are non-destructive inspection for medical and industrial diagnoses,[1–3] well logging,[4,5] and environmental monitoring.[6] The typical requirements for a scintillator are rapid decay, high light yield, high density (ρ), and large effective atomic number (Z_{eff}). To explore novel scintillators, the scintillation properties of inorganic materials have been investigated.[7–28]

To date, heavy scintillators have been developed because the interaction probability of photoabsorption depends on $\sim\rho Z_{eff}^4$.[29] For example, $Bi_4Ge_3O_{12}$ (BGO),[30] $PbWO_4$ (PWO),[31] Ce:$Lu_{(2-x)}Y_xSiO_5$ (LYSO),[32] and Pr:$Lu_3Al_5O_{12}$ (LuAG)[33] have been developed as X- and gamma-ray detection scintillators. However, the light yields of BGO (8200 photons/MeV)[34] and PWO (200 photons/MeV)[35] are relatively low, and LYSO and LuAG have radioisotopes of ^{176}Lu. Hf-based materials are attractive hosts for developing novel heavy scintillators due to

*Corresponding author: e-mail: fukushima.hiroyuki.ex8@ms.naist.jp
https://doi.org/10.18494/SAM4139

ISSN 0914-4935
https://myukk.org/

their high ρ and Z_{eff}. The melting points of Hf-based materials are over ~2400 °C; thus, their scintillation properties have been investigated for materials in a powder or ceramic form.[36–38] Single crystals of Hf-based materials have recently been grown by the floating zone (FZ) method.[39–42] In particular, the scintillation properties of perovskite-type hafnate single crystals have been investigated.[43,44]

Ce:$CaHfO_3$ single crystals have been grown from a Ca-rich composition because CaO is volatilized at the melting point of $CaHfO_3$.[45] The light yield of 3% Ce:$CaHfO_3$ is approximately 7800 photons/MeV, which is one of the highest values among the Hf-based oxide materials. To enhance the light yield, in this study, we focused on Mg-admixed crystals. $CaHfO_3$ single crystals have a Ca deficiency due to the volatilization of CaO, and the Ca deficiency may adversely affect scintillation properties. To compensate for the Ca deficiency, the addition of Mg at the Ca site is possible because the valence states of Mg and Ca are the same. In addition, MgO has a low vapor pressure; thus, Mg can be incorporated into the Ca site of $CaHfO_3$ single crystals. Moreover, the bandgap and the activator energy level of $CaHfO_3$ change upon replacement with Mg, and many successful results for the enhancement of light yield using admixed crystals have been reported.[46–48] In this study, the photoluminescence (PL) and scintillation properties of Ce:$(Mg_xCa_{1-x})HfO_3$ single crystals were investigated.

2. Materials and Methods

Ce:$(Mg_xCa_{1-x})HfO_3$ single crystals were synthesized using an FZ furnace equipped with four xenon lamps. The single-crystal growth conditions were the same as those of previously synthesized Ce:$CaHfO_3$ single crystals, and the concentration of Ce was fixed to 3 mol.%.[45] The nominal concentrations of Mg were 0.5, 2.5, 5, and 10 mol.% with respect to the Ca site. X-ray diffraction (XRD) patterns were measured in the range of 10–70° (Rigaku, MiniFlex600). Diffuse transmission spectra were recorded by a spectrophotometer (Shimadzu, Solidspec-3700). PL excitation and emission spectra were measured by a spectrofluorometer (JASCO, FP8600). The PL quantum yield (*QY*) was measured by a spectrometer (Hamamatsu Photonics, C11347). The PL decay curve was measured by a spectrometer (Hamamatsu Photonics, C11367). Scintillation spectra and decay curves were recorded using a laboratory-made setup.[49,50] The applied voltage and tube current during the measurement of the scintillation spectra were 40 kV and 1.2 mA, respectively. The pulse height distribution was measured by the same manner as previously reported.[49] As an irradiation source, ^{137}Cs gamma-rays (662 keV) were used. The reference crystal was BGO, and the light yield of BGO was calibrated to 6800 photons/MeV using a Si avalanche photodiode and an ^{55}Fe X-ray source.

3. Results and Discussion

Single crystals of Ce:$(Mg_xCa_{1-x})HfO_3$ were successfully synthesized by the FZ method. Figure 1 shows photographs and XRD patterns of Ce:$(Mg_xCa_{1-x})HfO_3$. The synthesized samples were colorless and transparent, and their length and thickness were approximately 3–5 and 1 mm, respectively. The remaining pieces of the samples were crushed for XRD measurement.

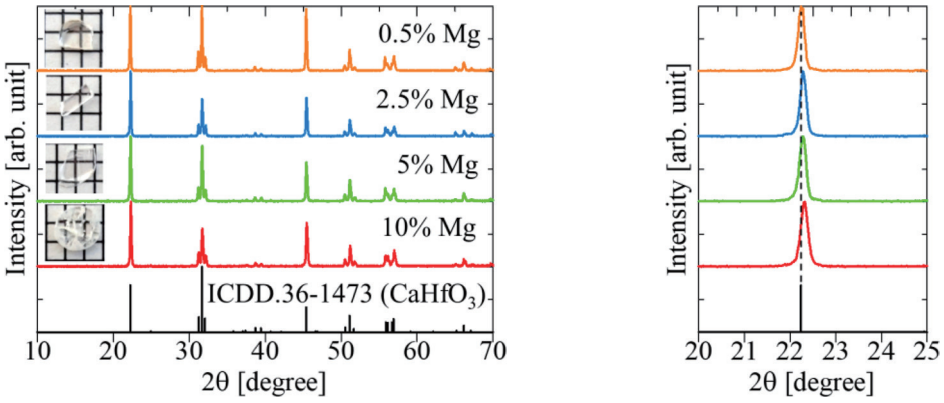

Fig. 1. (Color online) (a) XRD patterns and photographs of Ce:(Mg_xCa_{1-x})HfO_3 and (b) enlarged XRD patterns from 20 to 25°.

All XRD patterns of the samples were in good agreement with the reference XRD patterns of $CaHfO_3$ (ICDD. 36-1473). The peak position shifted to a higher angle with increasing Mg concentration because the ionic radii of Ca^{2+} in 12-old coordination and Mg^{2+} in eightfold coordination were 1.34 and 0.89 Å, respectively.[51] Since the maximum coordination number of Mg^{2+} was eight, Mg^{2+} may be substituted in an eight-coordinated form at the Ca^{2+} site.

Figure 2 shows the diffuse transmission spectra of Ce:(Mg_xCa_{1-x})HfO_3. The maximum transmittance was approximately 80% in the range of 400–800 nm. The cutoff wavelength due to the 4f–5d transition of Ce^{3+} was observed at ~375 nm, and the cutoff wavelength shifted to a longer wavelength with increasing concentration of Mg. The cutoff wavelength may be affected by Ce^{4+};[52] however, the ratio of Ce^{3+} to Ce^{4+} was unknown in this study. In future work, we should investigate the valence state of the doped Ce. The 5% Mg-admixed sample showed almost the same cutoff wavelength as that of the 0.5% Mg-admixed sample. When Ce^{3+} was substituted for Ca^{2+}, the coordination number of Ce^{3+} was 12. On the other hand, the coordination number of Ce^{3+} substituted for Mg^{2+} was considered to be eight. The crystal field strength was changed by the Mg substitution, and the 5d energy level of Ce^{3+} may also vary with the substitution site. Moreover, as mentioned above, the amount of Ce^{4+} may affect the cutoff wavelength. Therefore, the cutoff wavelength of the 5% Mg-admixed sample was shifted to a shorter wavelength.

Figure 3 shows the PL excitation and emission spectra of Ce:(Mg_xCa_{1-x})HfO_3. A broad luminescence band appeared at ~430 nm under the excitation wavelength of 340 nm. Excitation peaks were observed at 285 and 340 nm. A similar spectral feature has been observed in Ce:$CaHfO_3$ single crystals.[45] The Stokes shift of Ce:(Mg_xCa_{1-x})HfO_3 was 6155 cm^{-1}, which is larger than those of Ce-doped scintillators such as Ce:LYSO (2800 cm^{-1}),[53] Ce:$Lu_2Si_2O_7$ (2200 cm^{-1}),[53] and Ce:$Y_3Al_5O_{12}$ (3800 cm^{-1}).[54] The large Stokes shift of Ce:(Mg_xCa_{1-x})HfO_3 may lead to thermal quenching of the excited 5d level; thus, the temperature dependence on the scintillation properties of Ce:(Mg_xCa_{1-x})HfO_3 should be investigated in the future. The PL *QY*s of the 0.5, 2.5, 5, and 10% Mg-admixed samples were 40.5, 39.7, 50.5, and 38.2%, respectively.

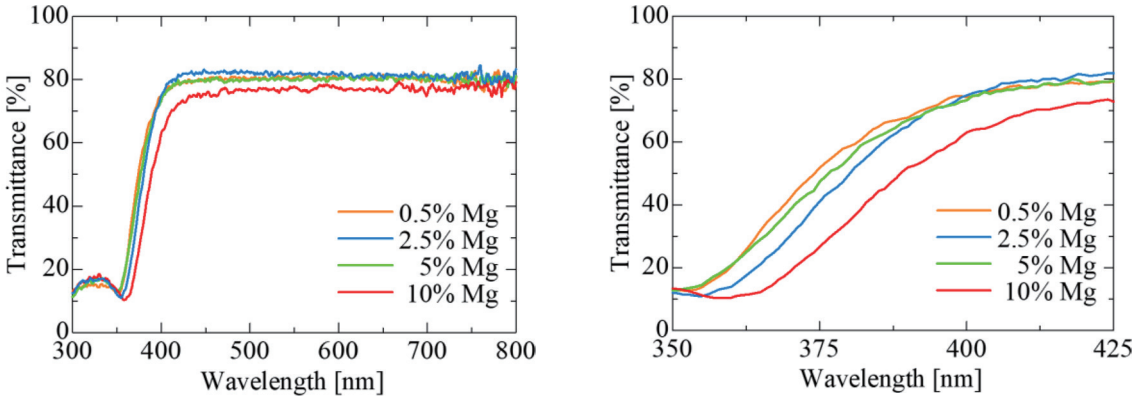

Fig. 2. (Color online) (a) Transmission spectra of Ce:(Mg_xCa_{1-x})HfO_3 and (b) enlarged transmission spectra from 350 to 425 nm.

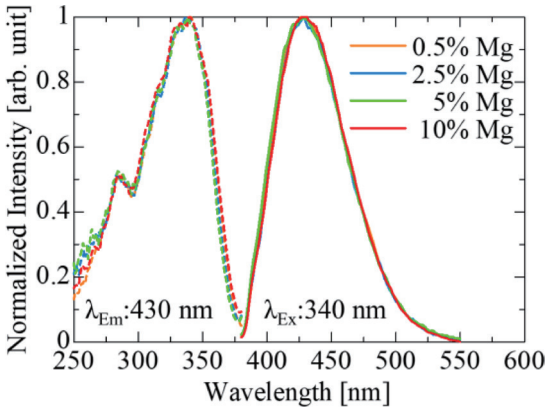

Fig. 3. (Color online) PL excitation and emission spectra of Ce:(Mg_xCa_{1-x})HfO_3.

The highest PL *QY* was observed for the 5% Mg-admixed sample, and the value was about twice that of the non-Mg-admixed Ce:$CaHfO_3$ single crystal.[45] The crystal field was changed by the Mg substitution, and the energy gap between the 5d energy level of Ce^{3+} and the bottom of the conduction band was optimized; thus improving the PL *QY*. Such manipulation of the energy gap has been reported.[55–57] Figure 4 shows the PL decay curves of Ce:(Mg_xCa_{1-x})HfO_3. The excitation and monitoring wavelengths were 340 and 430 nm, respectively. The observed decay curves were approximated by a sum of two exponential decay functions. Table 1 lists the PL decay time constants of Ce:(Mg_xCa_{1-x})HfO_3. The faster decay components (τ_1) were 20–22 ns and the slower decay components (τ_2) were 50–60 ns. The value of τ_1 was almost the same as that of non-Mg-admixed Ce:$CaHfO_3$ single crystals;[45] thus, the origin of τ_1 was the 5d–4f transition of Ce^{3+}. The slower decay component was observed in only the Mg-admixed samples, in which Ce^{3+} may substitute for Mg^{2+}. Considering the decay time constant and emission and excitation wavelengths, we concluded that the origin of τ_2 is also the 5d–4f transition of Ce^{3+} at Mg^{2+} sites.

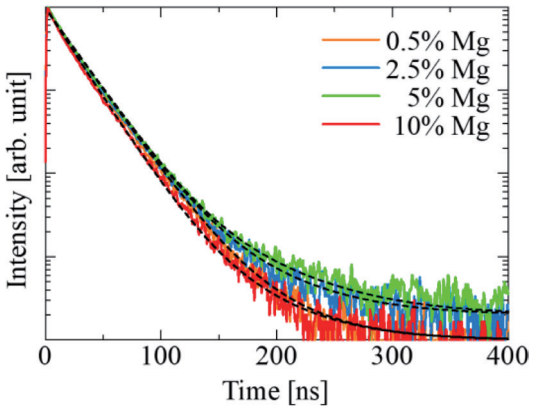

Fig. 4. (Color online) PL decay curves of Ce:(Mg_xCa_{1-x})HfO_3.

Table 1
PL and scintillation decay time constants of Ce:(Mg_xCa_{1-x})HfO_3.

Sample	PL decay time constants		Scintillation decay time constants	
	τ_1 (ns)	τ_2 (ns)	τ_1 (ns)	τ_2 (ns)
0.5% Mg	22 (98.8%)	50 (1.2%)	21 (96.4%)	261 (3.6%)
2.5% Mg	22 (98.2%)	55 (1.8%)	20 (95.4%)	222 (4.6%)
5% Mg	22 (98.2%)	60 (1.8%)	27 (93.7%)	291 (6.3%)
10% Mg	20 (98.8%)	50 (1.2%)	19 (96.0%)	232 (4.0%)

Figure 5 shows the X-ray-induced scintillation spectra of Ce:(Mg_xCa_{1-x})HfO_3. A broad luminescence band at ~430 nm was observed in all the samples. The peak wavelength was shifted to a longer wavelength in the 2.5 and 10% Mg-admixed samples due to self-absorption by the 4f–5d transition of Ce^{3+}. On the other hand, the 5% Mg-admixed sample exhibited no peak shift, which was consistent with the transmission spectra. Figure 6 shows the X-ray-induced scintillation decay curves of Ce:(Mg_xCa_{1-x})HfO_3. The observed decay curves were fitted by a sum of two exponential decay functions. Table 1 lists the scintillation decay time constants. The faster decay components (τ_1) and slower decay components (τ_2) were similar to those observed in Ce:$CaHfO_3$ single crystals.[45] Therefore, the origin of τ_1 and τ_2 was the 5d–4f transition of Ce^{3+} and host defects.

Figure 7 shows the afterglow curves of Ce:(Mg_xCa_{1-x})HfO_3. The afterglow level is defined as the intensity 20 ms after stopping X-ray exposure relative to the intensity during X-ray exposure. The obtained afterglow levels of the 0.5, 2.5, 5, and 10% Mg-admixed samples were 4800, 2300, 3000, and 2400 ppm, respectively. These values were smaller than those in non-Mg-admixed Ce:$CaHfO_3$.[45] Figure 8 exhibits the pulse height distribution of ^{137}Cs gamma-rays using Ce:(Mg_xCa_{1-x})HfO_3. All the samples exhibited a clear photoabsorption peak, and the light yields of the 0.5, 2.5, 5, and 10% Mg-admixed samples were 7800, 7800, 9500, and 3600 photons/MeV, respectively. The highest light yield was obtained for the 5% Mg-admixed sample, which showed the highest PL *QY* among the synthesized samples.

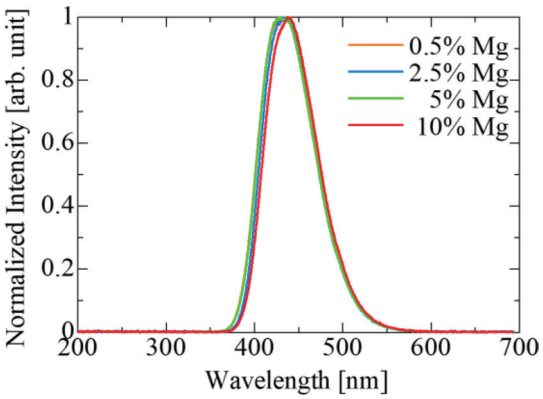

Fig. 5. (Color online) X-ray-induced scintillation spectra of Ce:(Mg_xCa_{1-x})HfO_3.

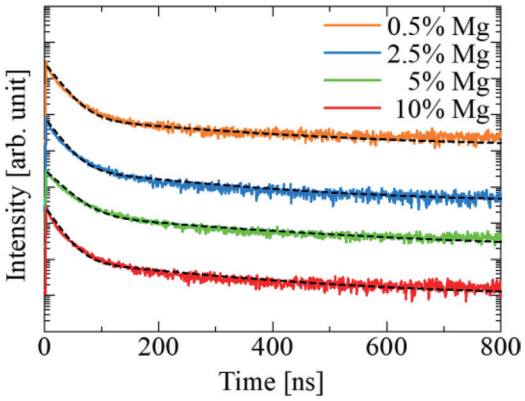

Fig. 6. (Color online) X-ray-induced scintillation decay curves of Ce:(Mg_xCa_{1-x})HfO_3.

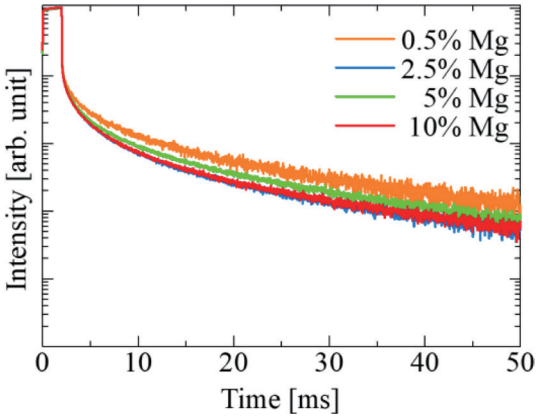

Fig. 7. (Color online) Afterglow curves of Ce:(Mg_xCa_{1-x})HfO_3.

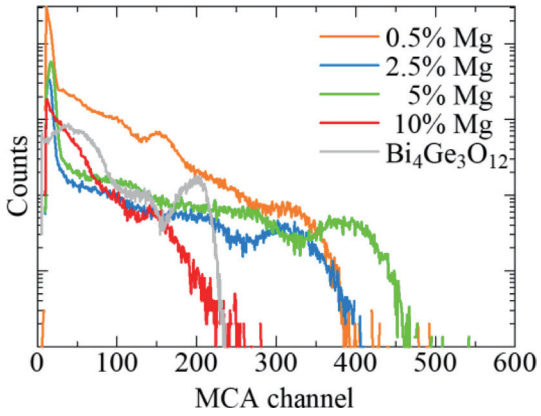

Fig. 8. (Color online) Pulse height distribution of 137Cs gamma-ray using Ce:(Mg_xCa_{1-x})HfO_3.

4. Conclusions

The PL and scintillation properties of Ce:(Mg_xCa_{1-x})HfO_3 single crystals were investigated. The Mg-admixed samples showed similar spectra to those observed for Ce:$CaHfO_3$ single crystals. The PL decay curves involved two decay components due to the 5d–4f transition of Ce^{3+} substituted at Ca^{2+} and Mg^{2+}. The PL *QY* was improved by Mg substitution, and the 5% Mg-admixed sample exhibited the highest PL *QY* among the samples. The scintillation spectra and decay curves were almost the same as that observed for Ce:$CaHfO_3$. The light yield was enhanced by Mg substitution, and the highest light yield of ~9500 photons/MeV was observed for the 5% Mg-admixed sample.

Acknowledgments

This work was supported by Grants-in-Aid for Scientific Research A (22H00309), Scientific Research B (21H03733, 21H03736, and 22H03872), Exploratory Research (22K18997), and JSPS Fellow (20J23226) from Japan Society for the Promotion of Science. JST A-STEP, Foundation from Cooperative Research Project of Research Center for Biomedical Engineering, Nippon Sheet Glass Foundation, Terumo Life Science Foundation, Iwatani Naoji Foundation, and Konica Minolta Science and Technology Foundation are also acknowledged.

References

1 T. Flohr, M. Petersilka, A. Henning, S. Ulzheimer, J. Ferda, and B. Schmidt: Phys. Medica **79** (2020) 126. https://doi.org/10.1016/j.ejmp.2020.10.030
2 G. Harding: Radiat. Phys. Chem. **71** (2004) 869. https://doi.org/10.1016/j.radphyschem.2004.04.111
3 T. K. Lewellen: Phys. Med. Biol. **53** (2008) R287. https://doi.org/10.1088/0031-9155/53/17/R01
4 C. L. Melcher: Nucl. Instrum. Methods Phys. Res., Sect. B **40**–**41** (1989) 1214. https://doi.org/10.1016/0168-583X(89)90622-8
5 T. Yanagida, Y. Fujimoto, S. Kurosawa, K. Kamada, H. Takahashi, Y. Fukazawa, M. Nikl, and V. Chani: Jpn. J. Appl. Phys. **52** (2013) 076401. https://doi.org/10.7567/JJAP.52.076401
6 S. Moriuchi, M. Tsutsumi, and K. Saito: Japanese J. Heal. Phys. **44** (2009) 122. https://doi.org/10.5453/jhps.44.122
7 T. Yanagida, Y. Fujimoto, H. Masai, G. Okada, T. Kato, D. Nakauchi, and N. Kawaguchi: Sens. Mater. **33** (2021) 2179. https://doi.org/10.18494/SAM.2021.3315
8 D. Nakauchi, T. Kato, N. Kawaguchi, and T. Yanagida: Sens. Mater. **33** (2021) 2203. https://doi.org/10.18494/SAM.2021.3323
9 D. Nakauchi, H. Fukushima, T. Kato, N. Kawaguchi, and T. Yanagida: Sens. Mater. **34** (2022) 611. https://doi.org/10.18494/SAM3696
10 P. Kantuptim, D. Nakauchi, T. Kato, N. Kawaguchi, and T. Yanagida: Sens. Mater. **34** (2022) 603. https://doi.org/10.18494/SAM3690
11 T. Kunikata, T. Kato, D. Shiratori, D. Nakauchi, N. Kawaguchi, and T. Yanagida: Sens. Mater. **34** (2022) 661. https://doi.org/10.18494/SAM3683
12 G. Ito, H. Kimura, D. Shiratori, D. Nakauchi, T. Kato, N. Kawaguchi, and T. Yanagida: Sens. Mater. **34** (2022) 685. https://doi.org/10.18494/SAM3681
13 K. Okazaki, D. Onoda, D. Nakauchi, N. Kawano, H. Fukushima, T. Kato, N. Kawaguchi, and T. Yanagida: Sens. Mater. **34** (2022) 575. https://doi.org/10.18494/SAM3678
14 D. Onoda, M. Akatsuka, N. Kawano, T. Kato, D. Nakauchi, N. Kawaguchi, and T. Yanagida: Sens. Mater. **34** (2022) 585. https://doi.org/10.18494/SAM3679
15 T. Kato, D. Nakauchi, N. Kawaguchi, and T. Yanagida: Sens. Mater. **34** (2022) 653. https://doi.org/10.18494/SAM3682
16 K. Ichiba, Y. Takebuchi, H. Kimura, D. Shiratori, T. Kato, D. Nakauchi, N. Kawaguchi, and T. Yanagida: Sens. Mater. **34** (2022) 677. https://doi.org/10.18494/SAM3680
17 H. Fukushima, D. Nakauchi, T. Kato, N. Kawaguchi, and T. Yanagida: Optik **238** (2021) 166789. https://doi.org/10.1016/j.ijleo.2021.166789
18 H. Fukushima, D. Nakauchi, T. Kato, N. Kawaguchi, and T. Yanagida: Opt. Mater. **128** (2022) 112385. https://doi.org/10.1016/j.optmat.2022.112385
19 H. Masai, T. Ina, H. Kimura, N. Kawaguchi, and T. Yanagida: Sens. Mater. **33** (2021) 2155. https://doi.org/10.18494/SAM.2021.3326
20 D. Shiratori, T. Kato, D. Nakauchi, N. Kawaguchi, and T. Yanagida: Sens. Mater. **33** (2021) 2171. https://doi.org/10.18494/SAM.2021.3317
21 H. Kimura, T. Kato, D. Nakauchi, N. Kawaguchi, and T. Yanagida: Sens. Mater. **33** (2021) 2187. https://doi.org/10.18494/SAM.2021.3322
22 N. Kawaguchi, H. Masai, M. Akatsuka, D. Nakauchi, T. Kato, and T. Yanagida: Sens. Mater. **33** (2021) 2215. https://doi.org/10.18494/SAM.2021.3410
23 M. Akatsuka, H. Kimura, D. Onoda, D. Shiratori, D. Nakauchi, T. Kato, N. Kawaguchi, and T. Yanagida: Sens. Mater. **33** (2021) 2243. https://doi.org/10.18494/SAM.2021.3319

24 P. Kantuptim, H. Fukushima, H. Kimura, D. Nakauchi, T. Kato, M. Koshimizu, N. Kawaguchi, and T. Yanagida: Sens. Mater. **33** (2021) 2195. https://doi.org/10.18494/SAM.2021.3316
25 H. Fukushima, M. Akatsuka, H. Kimura, D. Onoda, D. Shiratori, D. Nakauchi, T. Kato, N. Kawaguchi, and T. Yanagida: Sens. Mater. **33** (2021) 2235. https://doi.org/10.18494/SAM.2021.3324
26 M. Akatsuka, N. Daisuke, K. Takumi, N. Kawaguchi, and T. Yanagida: Sens. Mater. **34** (2022) 619. https://doi.org/10.18494/SAM3692
27 H. Kimura, T. Kato, D. Nakauchi, N. Kawaguchi, and T. Yanagida: Sens. Mater. **34** (2022) 691. https://doi.org/10.18494/SAM3687
28 T. Yanagida, T. Kato, D. Nakauchi, and N. Kawaguchi: Sens. Mater. **34** (2022) 595. https://doi.org/10.18494/SAM3684
29 T. Yanagida: Proc. Japan Acad. Ser. B **94** (2018) 75. https://doi.org/10.2183/pjab.94.007
30 M. J. Weber and R. R. Monchamp: J. Appl. Phys. **44** (1973) 5495. https://doi.org/10.1063/1.1662183
31 P. Lecoq, I. Dafinei, E. Auffray, M. Schneegans, M. V. Korzhik, O. V. Missevitch, V. B. Pavlenko, A. A. Fedorov, A. N. Annenkov, V. L. Kostylev, and V. D. Ligun: Nucl. Instrum. Methods Phys. Res., Sect. A **365** (1995) 291. https://doi.org/10.1016/0168-9002(95)00589-7
32 L. Pidol, A. Kahn-Harari, B. Viana, E. Virey, B. Ferrand, P. Dorenbos, J. T. M. De Haas, and C. W. E. Van Eijk: IEEE Trans. Nucl. Sci. **51** (2004) 1084. https://doi.org/10.1109/TNS.2004.829542
33 M. Kobayashi, S. Aogaki, F. Takeutchi, Y. Tamagawa, and Y. Usuki: Nucl. Instrum. Methods Phys. Res., Sect. A **693** (2012) 226. https://doi.org/10.1016/j.nima.2012.07.045
34 I. Holl, E. Lorenz, and G. Mageras: IEEE Trans. Nucl. Sci. **35** (1988) 105. https://doi.org/10.1109/23.12684
35 A. A. Annenkov, M. . Korzhik, and P. Lecoq: Nucl. Instrum. Methods Phys. Res., Sect. A **490** (2002) 30. https://doi.org/10.1016/S0168-9002(02)00916-6
36 A. Grezer, E. Zych, and L. Kpiński: Radiat. Meas. **45** (2010) 386. https://doi.org/10.1016/j.radmeas.2009.09.014
37 S. Derenzo, G. Bizarri, R. Borade, E. Bourret-Courchesne, R. Boutchko, A. Canning, A. Chaudhry, Y. Eagleman, G. Gundiah, S. Hanrahan, M. Janecek, and M. Weber: Nucl. Instrum. Methods Phys. Res., Sect. A **652** (2011) 247. https://doi.org/10.1016/j.nima.2010.09.156
38 I. Villa, F. Moretti, M. Fasoli, A. Rossi, B. Hattendorf, C. Dujardin, M. Niederberger, A. Vedda, and A. Lauria: Adv. Opt. Mater. **8** (2020) 1901348. https://doi.org/10.1002/adom.201901348
39 X. Xu, F. T. Huang, Y. Qi, S. Singh, K. M. Rabe, D. Obeysekera, J. Yang, M. W. Chu, and S. W. Cheong: Nat. Mater. **20** (2021) 826. https://doi.org/10.1038/s41563-020-00897-x
40 D. Nakauchi, G. Okada, N. Kawaguchi, and T. Yanagida: Jpn. J. Appl. Phys. **57** (2018) 100307. https://doi.org/10.7567/JJAP.57.100307
41 D. Nakauchi, T. Kato, N. Kawaguchi, and T. Yanagida: Sens. Mater. **32** (2020) 1389. https://doi.org/10.18494/SAM.2020.2751
42 D. Nakauchi, N. Kawaguchi, and T. Yanagida: Opt. Mater. **90** (2019) 227. https://doi.org/10.1016/j.optmat.2019.02.050
43 H. Fukushima, D. Nakauchi, N. Kawaguchi, and T. Yanagida: Jpn. J. Appl. Phys. **58** (2019) 052005. https://doi.org/10.7567/1347-4065/ab116c
44 H. Fukushima, D. Nakauchi, T. Kato, N. Kawaguchi, and T. Yanagida: Radiat. Meas. **133** (2020) 106280. https://doi.org/10.1016/j.radmeas.2020.106280
45 H. Fukushima, D. Nakauchi, T. Kato, N. Kawaguchi, and T. Yanagida: J. Lumin. **250** (2022) 119088. https://doi.org/10.1016/j.jlumin.2022.119088
46 O. Sidletskiy, A. Gektin, and A. Belsky: **2387** (2014) 2384. https://doi.org/10.1002/pssa.201431137
47 O. Sidletskiy, A. Belsky, A. Gektin, S. Neicheva, D. Kurtsev, V. Kononets, C. Dujardin, K. Lebbou, O. Zelenskaya, V. Tarasov, K. Belikov, and B. Grinyov: Cryst. Growth Des. **12** (2012) 4411. https://doi.org/10.1021/cg300608t
48 W. Drozdowski, K. Brylew, A. J. Wojtowicz, J. Kisielewski, M. Świrkowicz, T. Łukasiewicz, J. T. M. de Haas, and P. Dorenbos: Opt. Mater. Express **4** (2014) 1207. https://doi.org/10.1364/OME.4.001207
49 T. Yanagida, K. Kamada, Y. Fujimoto, H. Yagi, and T. Yanagitani: Opt. Mater. **35** (2013) 2480. https://doi.org/10.1016/j.optmat.2013.07.002
50 T. Yanagida, Y. Fujimoto, T. Ito, K. Uchiyama, and K. Mori: Appl. Phys. Express **7** (2014) 062401. https://doi.org/10.7567/APEX.7.062401
51 R. D. Shannon: Acta Crystallogr. Sect. A **32** (1976) 751. https://doi.org/10.1107/S0567739476001551
52 H. Masai, G. Okada, A. Torimoto, T. Usui, N. Kawaguchi, and T. Yanagida: Sci. Rep. **8** (2018) 623. https://doi.org/10.1038/s41598-017-18954-y
53 L. Pidol, A. Kahn-Harari, B. Viana, E. Virey, B. Ferrand, P. Dorenbos, J. T. M. de Haas, and C. W. E. van Eijk: IEEE Trans. Nucl. Sci. **51** (2004) 1084. https://doi.org/10.1109/TNS.2004.829542

54 G. Blasse and A. Bril: J. Chem. Phys. **47** (1967) 5139. https://doi.org/10.1063/1.1701771
55 J. Ueda, S. Tanabe, and T. Nakanishi: J. Appl. Phys. **110** (2011) 053102. https://doi.org/10.1063/1.3632069
56 D. Nakauchi, G. Okada, N. Kawano, N. Kawaguchi, and T. Yanagida: Jpn. J. Appl. Phys. **57** (2018) 02CB02. https://doi.org/10.7567/JJAP.57.02CB02
57 J. Ueda, A. Meijerink, P. Dorenbos, A. J. J. Bos, and S. Tanabe: Phys. Rev. B **95** (2017) 014303. https://doi.org/10.1103/PhysRevB.95.014303